ELSEVIER

Nuclear Instruments and Methods in Physics Research B 166–167 (2000) 949–953

NIM B
Beam Interactions with Materials & Atoms

www.elsevier.nl/locate/nimb

Tracks induced in TeO_2 by heavy ions at low velocities

G. Szenes [a,*], F. Pászti [b], Á. Péter [c], A.I. Popov [d,e]

[a] *Department of General Physics, Eötvös University, P.O.B. 32, H-1518 Budapest, Hungary*
[b] *Research Institute for Particle and Nuclear Physics, Konkoly-Thege út 29-33, 1121 Budapest, Hungary*
[c] *Research Institute for Solid State Physics and Optics, Konkoly-Thege út 29-33, 1121 Budapest, Hungary*
[d] *CIRIL, Lab. CEA/CNRS, rue Claude Bloch, BP 5133, 14040 Caen Cedex, France*
[e] *Institute of Solid State Physics, University of Latvia, 8 Kengaraga iela, LV-1063 Riga, Latvia*

Abstract

On the basis of its thermal properties, TeO_2 crystal was selected as an insulator with low threshold electronic stopping power for track formation S_{et}. The crystals were irradiated by S, Zn, Mo, Kr, Te and Pb ions and the optical absorption and track formation were studied. Comparison is made with the published results on $LiNbO_3$, $Y_3Fe_5O_{12}$ and SiO_2 quartz. Good quantitative agreement is found with the predictions of the thermal spike model of Szenes with respect to S_{et} and the variation of the track size with the electronic stopping power S_e. It is shown that TeO_2 has a high efficiency g at low ion velocities, which is a characteristic feature of the damage cross-section velocity effect.

PACS: 61.80.Az; 61.80.Jh; 61.82.Ms; 78.20-e
Keywords: Swift ions; Tracks; Thermal spike; RBS; Optical absorption

1. Introduction

As a result of the interaction of energetic ions with solids, tracks are formed. These tracks can be revealed by chemical etching, by electron microscopy, by Rutherford backscattering and by other methods. The size and the shape of these tracks are characteristic to the ion–solid interaction and to the process of deexcitation, as well. By studying the variation of the track sizes in the dependence of the ion energy and various target parameters we can get information about these points and check the present ideas.

Track formation is often explained by the thermal spike model of Toulemonde et al. [1]. Recently we showed that this model cannot explain the variation of the track size with the ion velocity (velocity effect) and the fitting parameter λ serves in this model mainly to compensate the quantitative consequences of the "drastic approximations" of the model [2]. Therefore, the physical meaning of the experimental value of the λ parameter is rather doubtful [3,4]. In [5] we proposed a phenomenological thermal spike model of track formation. The model predicts a simple relation

* Corresponding author. Tel.: +36-1-372-2821; fax: +36-1-372-2811.
E-mail address: szenes@ludens.elte.hu (G. Szenes).

0168-583X/00/$ - see front matter
PII: S0168-583X(99)01042-3

between the macroscopic thermal properties of solids and the threshold electronic stopping power for the formation of amorphous tracks S_{et}. We selected some insulators with such parameters, which ensure low S_{et}. By studying tracks in these materials we intend to check the expression for S_{et} and also the analytical equations of the model describing the evolution of tracks. In this paper we report the first results on TeO_2.

2. Experimental

Optical absorption measurements were performed with a double-beam Perkin Elmer spectrophotometer on TeO_2 samples irradiated by Mo, S and Te ions with initial energies of 8.67, 11.3 and 3.5 MeV/nucleon. The TeO_2 single crystals were grown in the Research Institute for Solid State Physics and Optics (Budapest). The optical absorption was measured in the 200–900 nm range as a function of the fluence and the electronic stopping power. No absorption bands were observed in the wavelength range from the absorption edge (290 nm, corresponding to the band gap of 4.3 eV) up to the near IR. Only fluence-dependent red-shift of the absorption edge and the appropriate increase of the absorption pedestal were seen.

The specimens for track studies were irradiated by Pb, Kr, Zn, and S ions with an initial energy of 4.5, 9.8, 9.0 and 11.3 MeV/nucleon, respectively. The beam energy was reduced by aluminium degrader foils to $E < 2.2$ MeV/nucleon. All irradiations were performed at room temperature at the GANIL (Caen, France) accelerator. The ion beam was scanned over a surface of about 6 cm^2 to ensure homogeneous irradiation conditions. The flux was kept around (2–4) $\times 10^8$ ions/cm^2s to avoid beam heating effects.

The irradiated crystals were investigated by Rutherford backscattering in channeling geometry (c-RBS) in the Research Institute for Particle and Nuclear Physics (Budapest). Measurements were made at different fluences and the effective track radii R_e were determined by applying the Poisson law. The experimental error of the track radii is about 10%. A considerable fraction of this error is due to the uncertainty in the fluence of swift ions. In insulators R_e is usually equal to the average radius of the amorphous cylinders. We assume that this is also valid for TeO_2. In the future this should be confirmed by electron microscopy.

The experimental data for TeO_2 are plotted in Fig. 1. A line going through the origin provides a good description of the track evolution in the given range. For comparison we also depicted in the figure the data for yttrium iron garnet (YIG) [2,6], lithium niobate (LN) [7] and SiO_2 quartz [8,9], which were obtained by monoatomic or cluster ion irradiation for $E < 2.2$ MeV/nucleon. These experimental data are so close to each other that it is reasonable to draw a single line through them. The figure clearly demonstrates that the track evolution in TeO_2 is much faster than in YIG, LN or SiO_2 quartz. The track induced by $E = 1.84$ MeV/nucleon Pb ions in TeO_2 has a larger diameter than the tracks measured in YIG after 40.2 MeV C_{60} bombardment. According to our knowledge, this is the largest track ever observed in any solids. Below we shall explain what is the reason that the track evolution is so similar in the three most frequently studied insulators, and why are the tracks about three times larger in TeO_2 at the same energy deposition.

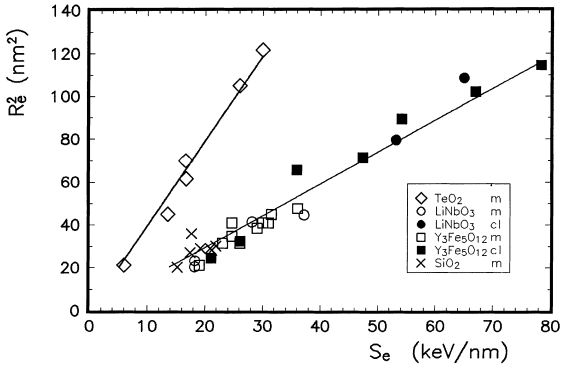

Fig. 1. Variation of the track size with S_e for irradiation with monoatomic (m) and cluster (cl) ions with $E < 2.2$ MeV/nucleon.

3. Discussion

The changes observed in the optical spectra are related to the simple light-diffusion effect resulting from the structural modifications induced by heavy-ion bombardment. A similar picture has been observed in $LiNbO_3$ [10] and $KNbO_3$ [11]. It is interesting to note that in MgO and Al_2O_3, F-type centres can be created not only by electron irradiation [12,13], but by irradiation with various ions, as well [14–16]. We attribute the different behavior of TeO_2 to the ionization-induced annealing of Frenkel pairs. In TeO_2 the annealing of close Frenkel defects should be highly effective, due to very low oxygen vacancy migration energy of 0.42–0.54 eV [17], with appropriate migration temperature very close to room temperature (i.e. below 100°C). Probably the same is valid for $KNbO_3$, where oxygen vacancy migration energy is 0.7 eV [18].

The results of track measurements were analyzed by the thermal spike model of Szenes, using the following three equations [5]:

$$R_e^2 = a^2(0)\ln(S_e/S_{et}) \quad \text{for } S_e < 2.7S_{et}, \tag{1}$$

$$R_e^2 = a^2(0)S_e/(2.7S_{et}) \quad \text{for } S_e > 2.7S_{et}, \tag{2}$$

$$S_{et} = \pi\rho c T_0 a^2(0)/g, \tag{3}$$

where ρ, c and T_0 denote the density, average specific heat, the difference between the melting point T_m and the irradiation temperature T_{ir}, respectively, and gS_e is the fraction of the electronic excitation transferred to the thermal spike (g-efficiency). The parameter $a(0)$ denotes the initial Gaussian width of the temperature distribution at the moment, when the peak temperature is the highest. S_{et} and $a^2(0)$ are the parameters of the model, which can be simply determined from the experimental data.

These equations have been applied to all systematic track data reported in the literature. The analysis showed that $a(0) = 4.5$ nm for all insulators studied so far [5], and there are evidences that the value of $a(0)$ does not depend on the specific ion energy E [4]. On the other hand, the efficiency g considerably varies with E in the range $0.17 < g < 0.5$ and this is the origin of the velocity effect.

The linear relation between R_e^2 and S_e required by Eq. (2) obviously fulfils for TeO_2 and YIG. There is a good agreement between the track data of YIG, LN and SiO_2 and later we show that this is the direct consequence of Eqs. (2) and (3). Previously, there was no possibility to quantitatively check Eq. (2), because at low ion velocities the few track data with $R_e < a(0)$ – available in publications – were not sufficient to determine the value of S_{et} for any insulators. On the other hand, at high ion velocities the lack of sufficient data with $R_e > a(0)$ was the difficulty.

Recently, experiments were performed on LN [7] and YIG [19] samples with beams of small cluster ions. From the analysis of these results we found at low ion velocities that $S_{et} = 4.6$ keV/nm for LN [4]. Jensen et al. induced amorphous tracks with $R_e < a(0)$ in YIG samples by C_5 and C_{10} cluster ions. Eq. (1) can be nicely fitted to the data providing $S_{et} = 6.3$ keV/nm.

A source of uncertainty is that S_{et} for YIG was determined by clusters in the range of $0.33 > E > 0.045$ MeV/nucleon where the value of the efficiency is not known from other experiments. In some irradiation experiments by monoatomic beams, we found an indication that a drop of the efficiency g may exist for $E < 0.8$ MeV/nucleon, that has not been confirmed yet [3]. Presently, experiments are in progress to clarify this point.

Eq. (3) is an important result of our thermal spike model. It is a relation between the macroscopic thermal properties of the target and its threshold electronic stopping power for amorphous track formation. We have shown that this relation is valid at high ion velocities ($E > 7.6$ MeV/nucleon) for various magnetic insulators [5]. We made estimates by applying Eq. (3) (S'_{et}) and Eq. (2) (S^*_{et}) and taking $a(0) = 4.5$ nm. The results are given in Table 1. together with the experimental values S^{ex}_{et} and the values of the physical parameters which were used in the calculations. S^{ex}_{et} values were determined according to Eq. (1) by the extrapolation of the experimental R_e^2–lnS_e curves to $R_e^2 = 0$. This procedure gives systematically higher S^{ex}_{et} values compared to the extrapolation from an R_e–S_e curve [6,8].

Table 1
The melting point T_m, the irradiation temperature T_{ir} and the average specific heat c for some insulating crystals (ρ is the density)[a]

	T_m (K)	T_{ir} (K)	c (kJ/kgK)	ρcT_0 (eV/nm^3)	S'_{et} (keV/nm)	S^*_{et} (keV/nm)	S^{ex}_{et} (keV/nm)
$LiNbO_3$	1523	300	0.85	29.4	4.67	5.05	4.6
$Y_3Fe_5O_{12}$	1790	300	0.67	32.4	5.15	5.05	6.3
SiO_2	1996	300	1.02	28.1	4.46	5.05	4.0
TeO_2	1006	300	0.47	12.34	1.96	1.87	–

[a] S^{ex}_{et} is an experimental value, S'_{et} and S^*_{et} were calculated according to Eqs. (3) and (2), respectively, by taking $g = 0.4$ and $a(0) = 4.5$ nm.

There is an excellent agreement between the two methods of calculation. The agreement is also good between the S^{ex}_{et} and S'_{et} values. The larger deviations for YIG may be related to the drop of the efficiency g for $E < 0.8$ MeV/nucleon [3]. The estimate provides for TeO_2 $S_{et} = 1.87$ keV/nm, which is the lowest value for insulating crystals.

If Eqs. (2) and (3) are combined we get

$$R_e^2 = gS_e/(2.7\pi\rho cT_0) \quad \text{for} \quad S_e > 2.7S_{et}. \tag{4}$$

According to this equation the slope of the lines in Fig. 1 is inversely proportional to ρcT_0. The ρcT_0 values are given in Table 1, and they are very close for SiO_2, LN and YIG. This is in excellent agreement with the plot in Fig. 1, where track evolution in these three materials have very close courses.

In a range where the efficiency is approximately constant $g \approx 0.4$ [4], Eq.(4) predicts a linear R_e^2–$S_e/\rho cT_0$ dependence with a slope $m = g/2.7\pi = 0.047$. This plot is shown in Fig. 2 and the variation of the track size with S_e in the four crystals clearly follows this theoretical line.

When the two plots are compared with the data in Table 1, it becomes evident that the governing materials parameter of track formation is ρcT_0, which is equal to the energy necessary to heat up the unit volume of the target to its melting temperature. Whatever the thermal diffusivity, electron–phonon coupling or the strength of the target are, the track evolution is affected only by ρcT_0. If low energy deposition is sufficient for melting – like in TeO_2 – then S_{et} is small and large tracks are induced. The track evolution is similar in materials with close values of ρcT_0 (YIG, LN, SiO_2 quartz). These results clearly show the importance of the thermal effects in the processes of track formation.

As $a(0) = 4.5$ nm for crystalline insulators, S_{et} and track sizes can be reliably estimated from the macroscopic properties by applying Eqs. (1)–(3) at low and high ion velocities where most information is available on the efficiency values.

It has been observed that low velocity ions are more efficient for track formation than high velocity ions [6]. At low ion velocities $g = 0.4$, which is more than two times higher than the efficiency at high ion velocities ($g = 0.17$) [3,4]. It has been previously known that SiO_2 quartz, LN and YIG exhibit the so-called velocity effect. The plot in Fig. 2 is a clear evidence that TeO_2 has also high efficiency at low ion velocities, thus it also exhibit the velocity effect.

Meftah et al., claimed in [2,20], that the band gap energy E_g largely affects track formation in insulators. One cannot observe any sign of such a dependence in Fig. 2 where the track data follow the same line in the normalized plot whatever is their gap energy. On the other hand, the R_e^2–S_e

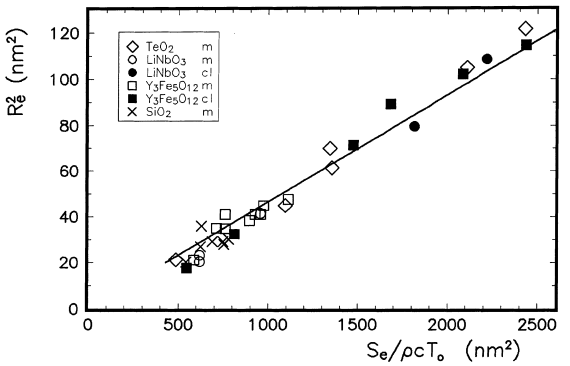

Fig. 2. The same data as in Fig. 1 in a normalized plot. The theoretical line has a slope $m = g/2.7\pi = 0.047$ assuming $g = 0.4$ (see Eq. (4)).

curves are very close for SiO_2, LN and YIG in Fig. 1 in spite of the fact, that their gap energies are rather different: $E_g = 12, 4.5$ and 2.8 eV, respectively. We do not know any experimental fact, which would indicate, that E_g is a relevant parameter of track formation in insulators.

4. Summary

No new optical bands are formed in irradiated TeO_2 crystal, which is explained by the annealing of close Frenkel pairs. TeO_2 crystals exhibit the damage cross-section velocity effect and the large tracks are in agreement with the predictions of the thermal spike model of Szenes. The governing materials parameter of track formation is $\rho c T_0$. The validity of Eq. (3), offering a relation between the macroscopic properties and S_{et}, is supported by the experimental results on TeO_2, LN, SiO_2 quartz and YIG. The agreement is good between the estimates of S_{et} made by applying Eqs. (2) and (3) using track data with $R_e > 4.5$ nm. The band gap energy has no effect on the values of S_{et} and on the R_e^2–S_e relation for $R_e > 4.5$ nm.

Acknowledgements

For their assistance in the experiments the authors are grateful to the staff of the CIRIL (Caen), especially to Dr. E. Balanzat, with whom we also had valuable discussions on the interpretation of the optical experiments. The partial support of the National Scientific Research Fund (OTKA, Hungary) is gratefully aknowledged by G.Sz. (contracts T025805 and T029701) and by P.F. (contract T025928).

References

[1] M. Toulemonde et al., Nucl. Instr. and Meth. B 116 (1996) 37.
[2] A. Meftah et al., Nucl. Instr. and Meth. B 122 (1997) 470.
[3] G. Szenes, Nucl. Instr. and Meth. B 146 (1998) 420.
[4] G. Szenes, Phys. Rev. B 60 (1999) 3140.
[5] G. Szenes, Phys. Rev. B 51 (1995) 8026.
[6] A. Meftah et al., Phys. Rev. B 48 (1993) 920.
[7] B. Canut, S.M.M. Ramos, Rad. Eff. Def. Solids 147 (1998) 1.
[8] A. Meftah et al., Phys. Rev. B 49 (1994) 12457.
[9] C. Trautmann, J.M. Costantini, A. Meftah, K. Schwartz, J.P. Stoquert, M. Toulemonde, in: J.C. Barbour, S. Roorda, D. Ila, M. Tsujioka, (Eds.), Atomistic Mechanisms in Beam Synthesis and Irradiation of Materials, MRS Symposium Proceedings No. 504, Materials Research Society, Warrendale, 1999, p. 123.
[10] B. Canut, R. Brenier, A. Meftah, P. Moretti, S. Ould Salem, S.M.M. Ramos, Thevenard, M. Toulemonde, Nucl. Instr. and Meth. B 91 (1994) 312.
[11] A.I. Popov, E. Balanzat, Unpublished.
[12] Y. Chen, D.L. Trueblod, O.E. Schow, H.T. Tohver, J. Phys. C 3 (1970) 2501.
[13] W.D. Compton, G.W. Arnold, Disc. Faraday Soc. 31 (1961) 130.
[14] B.D. Evans, Phys. Rev. B 9 (1974) 5222.
[15] B. Canut, A. Benyagub, G. Marest, A. Meftah, N. Moncoffre, S.M.M. Ramos, F. Studer, P. Thevenard, M. Toulemonde, Phys. Rev. B 51 (1995) 12194.
[16] R.S. Averback, P. Ehrhart, A.I. Popov, A.V. Sambeek, Rad. Eff. Def. Solids 136 (1995) 169.
[17] H. Jain, A.S. Nowick, Phys. Stat. Solidi A 67 (1981) 701.
[18] E. Kotomin, private comunication.
[19] J. Jensen, A. Dunlop, S. Della-Negra, M. Toulemonde, Nucl. Instr. and Meth. B 146 (1998) 412.
[20] A. Meftah et al., Mater Sci. Forum 248–249 (1997) 53.